RESEARCH ARTICLE

Effect of Surface-Modification on In Vitro Corrosion of Biodegradable Magnesium-Based Helical Stent Fabricated by Photo-chemical Etching

Authors

B S P K Kandala[1], G Zhang[1], X An[4], S Pixley[2], V Shanov[1,3*]

Affiliations

[1] Department of Mechanical and Materials Engineering, University of Cincinnati, OH 45221.

[2] Department of Pharmacology and Systems Physiology, University of Cincinnati, OH 45221.

[3] Department of Chemical and Environmental Engineering, University of Cincinnati, OH 45221.

[4] Department of Pharmaceutical Sciences, University of Cincinnati, OH 45221.

Correspondence

V Shanov
Department of Chemical and Environmental Engineering, University of Cincinnati, OH 45221
shanovvn@ucmail.uc.edu

Abstract

During the last decade, magnesium and its alloys have been extensively studied to develop a new generation of biodegradable medical implants. The fast degradation rate of pure magnesium and related alloys in the physiological environment poses significant challenges to devices made of these materials for biomedical applications. In this study, we have designed and fabricated biodegradable helical stents made of AZ31 magnesium alloy, and have explored theirs in vitro corrosion behavior in Dulbecco's Modified Eagle's Medium (DMEM). The corrosion rate was significantly reduced by surface modifications of the helical stent, achieved through applying a biocompatible Parylene C polymer coating, or via chemical etching of the devices in inorganic solutions. The corrosion rates of the coated AZ31 Mg helical stents were compared, with uncoated samples used as a control. The results achieved indicated that all tested surface modifications successfully inhibited metal corrosion rates in vitro. Materials coated with Parylene C coating revealed a maximum corrosion rate reduction of 70% to 85% in DMEM solution.

1. Introduction

During the past years, cardiovascular diseases have claimed more lives in the United States than any other cause of death [1]. Atherosclerosis is one progressive heart disease that usually afflicts the coronary, carotid, and femoral arteries, as well as the abdominal aorta [2]. This happens when excessive cholesterol deposits on the walls of the blood vessels, thus restricting the blood flow. The current treatment options include angioplasty, stenting, and bypass surgery. Combining angioplasty with stenting is now the preferred method to treat atherosclerotic plaques and lesions. Stents are cylindrically shaped devices with appropriate wall patterns that are used to dilate blood vessels by pushing plaques against the vessel walls, thereby maintaining a balanced blood flow without any constriction. Stents can be fabricated using different materials, like non-degradable or biodegradable metals, as well as biopolymers. These stents, in the physiological environment, are subjected to various types of mechanical loading conditions such as cyclic fatigue, shear stress caused by the high-velocity blood flow and viscosity of the blood. Also, the long-term presence of stents may lead to thrombosis, inflammation, and smooth muscle cell proliferation, which then are likely to lead to in-stent restenosis and neointimal hyperplasia. There are many factors that contribute to stent failures, such as disturbances in blood flow patterns, strut thickness, the shape of the stents, the residual mechanical stress from the manufacturing process, and restenosis. It has been shown that the device design is a major risk factor for restenosis in bare-metal stents [3].

Medical grade metals such as stainless steel, cobalt, and titanium-based alloys, are widely used in the market to produce biomedical implants. These materials possess high strength and good ductility. Due to the very low corrosion rates, they stay permanently in the human body and, in some cases, require explantation, which can be traumatic to the patients and may increase mortality, as well as the cost of the treatment [4,5].

Biodegradable metals such as magnesium, zinc and their alloys, are appropriate candidates to replace the commercial, non-degradable materials used currently to fabricate medical implants. Magnesium is the fourth most abundant element in the human body and it is primarily distributed in bone tissues [6]. The recommended daily dosage is 310 mg and 400 mg for adult males and females, respectively [7]. It was reported that magnesium-based implants can stimulate the development of hard callouses at fracture sites (a precursor to bone formation) [8]. Magnesium and its alloys possess unique mechanical properties that are closer to those of bone tissue than those of inert metals, including a Mg density of 1.7-2.0 g cm^{-3}, an elastic module of 41-45 GPa, and similar compressive and tensile strength. This enables magnesium and its alloys to stand out from other biomaterials for certain medical implant applications.

Numerous studies have reported that blood flow through arteries is laminar and spiral [9]. Physiologically, blood flow is spiral in nature because of the twisted nature of the heart on its axis and tapered, curved aortic arch.[10]. During coronary artery bypass surgery, it was shown that blood appeared to ‘rotate in a clockwise direction’, as registered by ultrasound measurement of blood velocities across the ascending aorta [11]. "Secondary spiral flow patterns" have been observed in the ascending aorta and at bifurcations [12]. A rotational nature of blood-

flow has also been reported in the descending thoracic aorta [9]. The above statements lead to the conclusion that the blood flow pattern in the arteries is spiral, laminar and is propagated as a result of the anatomy of arteries and positioning of the heart.

A spiral flow through arteries preserves the blood vessels from damage, by reduction of laterally directed forces. There are reports showing that stenting arteries with the conventional cylindrically devices, disturbs the natural blood flow and causes intimal hyperplasia [13,14]. This leads to blood coagulation (creating vessel-clogging clots), and damage to the intima, which is the layer of endothelial cells lining blood vessels. The advantages of helical spiral stents have been shown to be good expandability, flexibility and uniform expansion without kinking [15]. Researchers have suggested using a non-degradable helical centerline stent to restore the nature of the blood flow and prevent intimal hyperplasia [13]. A helical stent with a specific 3D geometric curvature will enable stimulation of swirling flow and reduction of wall shear stress [14]. Our group has designed, fabricated and tested a biodegradable metal stent with a helical shape. The results have been published by previously [16,17]. Bio-degradable metallic helical stents have the potential to overcome some current issues with conventionally shaped stents, such as limited expandability and high manufacturing costs. The helical stent discussed in this work was fabricated by a patented photo-chemical etching method, from a 2-dimensional Mg-AZ31 ribbon, followed by coiling it into a helical structure [18].

In vitro and ex vivo corrosion behaviors of magnesium stents made of the AZ31 alloy by photo-chemical etching, have been reported by our group [19–21]. Other studies that have tested magnesium alloys as bone implants, such as screws, plates, or other orthopedic fixture devices, have reported that magnesium-based implants showed good biocompatibility, with no change in cancellous tissues and no inflammation [22–24]. However, all magnesium implants still face the challenges of fast corrosion and the production of hydrogen release needs to be addressed. Corrosion control can be achieved by altering the surface of the Mg biodegradable implants through polymer coatings, as demonstrated in our previous studies [17,19]. The coating that we explored previously, and continue to test in this report, is Parylene C, which is a Food Drug & Administration (FDA) approved biocompatible polymer. It is a transparent, crystalline thermoplastic, and elastic polymer. Parylene C was also chosen because of its hydrophobic nature and low permeability. In the present research, we investigated how surface modification with two inorganic solutions and with a Parylene C coating affect the corrosion rate of AZ31 helical stents in vitro.

2. Materials and Methods

2.1. Fabrication of Helical Stents

1. Introduction

During the past years, cardiovascular diseases have claimed more lives in the United States than any other cause of death [1]. Atherosclerosis is one progressive heart disease that usually afflicts the coronary, carotid, and femoral arteries, as well as the abdominal aorta [2]. This happens when excessive cholesterol deposits on the walls of the blood vessels, thus restricting the blood flow. The current treatment options include angioplasty, stenting, and bypass surgery. Combining angioplasty with stenting is now the preferred method to treat atherosclerotic

plaques and lesions. Stents are cylindrically shaped devices with appropriate wall patterns that are used to dilate blood vessels by pushing plaques against the vessel walls, thereby maintaining a balanced blood flow without any constriction. Stents can be fabricated using different materials, like non-degradable or biodegradable metals, as well as biopolymers. These stents, in the physiological environment, are subjected to various types of mechanical loading conditions such as cyclic fatigue, shear stress caused by the high-velocity blood flow and viscosity of the blood. Also, the long-term presence of stents may lead to thrombosis, inflammation, and smooth muscle cell proliferation, which then are likely to lead to in-stent restenosis and neointimal hyperplasia. There are many factors that contribute to stent failures, such as disturbances in blood flow patterns, strut thickness, the shape of the stents, the residual mechanical stress from the manufacturing process, and restenosis. It has been shown that the device design is a major risk factor for restenosis in bare-metal stents [3].

Medical grade metals such as stainless steel, cobalt, and titanium-based alloys, are widely used in the market to produce biomedical implants. These materials possess high strength and good ductility. Due to the very low corrosion rates, they stay permanently in the human body and, in some cases, require explantation, which can be traumatic to the patients and may increase mortality, as well as the cost of the treatment [4,5].

Biodegradable metals such as magnesium, zinc and their alloys, are appropriate candidates to replace the commercial, non-degradable materials used currently to fabricate medical implants. Magnesium is the fourth most abundant element in the human body and it is primarily distributed in bone tissues [6]. The recommended daily dosage is 310 mg and 400 mg for adult males and females, respectively [7]. It was reported that magnesium-based implants can stimulate the development of hard callouses at fracture sites (a precursor to bone formation) [8]. Magnesium and its alloys possess unique mechanical properties that are closer to those of bone tissue than those of inert metals, including a Mg density of 1.7-2.0 g cm^{-3}, an elastic module of 41-45 GPa, and similar compressive and tensile strength. This enables magnesium and its alloys to stand out from other biomaterials for certain medical implant applications.

Numerous studies have reported that blood flow through arteries is laminar and spiral [9]. Physiologically, blood flow is spiral in nature because of the twisted nature of the heart on its axis and tapered, curved aortic arch.[10]. During coronary artery bypass surgery, it was shown that blood appeared to ‘rotate in a clockwise direction’, as registered by ultrasound measurement of blood velocities across the ascending aorta [11]. "Secondary spiral flow patterns" have been observed in the ascending aorta and at bifurcations [12]. A rotational nature of blood-flow has also been reported in the descending thoracic aorta [9]. The above statements lead to the conclusion that the blood flow pattern in the arteries is spiral, laminar and is propagated as a result of the anatomy of arteries and positioning of the heart.

A spiral flow through arteries preserves the blood vessels from damage, by reduction of laterally directed forces. There are reports

showing that stenting arteries with the conventional cylindrically devices, disturbs the natural blood flow and causes intimal hyperplasia [13,14]. This leads to blood coagulation (creating vessel-clogging clots), and damage to the intima, which is the layer of endothelial cells lining blood vessels. The advantages of helical spiral stents have been shown to be good expandability, flexibility and uniform expansion without kinking [15]. Researchers have suggested using a non-degradable helical centerline stent to restore the nature of the blood flow and prevent intimal hyperplasia [13]. A helical stent with a specific 3D geometric curvature will enable stimulation of swirling flow and reduction of wall shear stress [14]. Our group has designed, fabricated and tested a biodegradable metal stent with a helical shape. The results have been published by previously [16,17]. Bio-degradable metallic helical stents have the potential to overcome some current issues with conventionally shaped stents, such as limited expandability and high manufacturing costs. The helical stent discussed in this work was fabricated by a patented photo-chemical etching method, from a 2-dimensional Mg-AZ31 ribbon, followed by coiling it into a helical structure [18].

In vitro and ex vivo corrosion behaviors of magnesium stents made of the AZ31 alloy by photo-chemical etching, have been reported by our group [19–21]. Other studies that have tested magnesium alloys as bone implants, such as screws, plates, or other orthopedic fixture devices, have reported that magnesium-based implants showed good biocompatibility, with no change in cancellous tissues and no inflammation [22–24]. However, all magnesium implants still face the challenges of fast corrosion and the production of hydrogen release needs to be addressed. Corrosion control can be achieved by altering the surface of the Mg biodegradable implants through polymer coatings, as demonstrated in our previous studies [17,19]. The coating that we explored previously, and continue to test in this report, is Parylene C, which is a Food Drug & Administration (FDA) approved biocompatible polymer. It is a transparent, crystalline thermoplastic, and elastic polymer. Parylene C was also chosen because of its hydrophobic nature and low permeability. In the present research, we investigated how surface modification with two inorganic solutions and with a Parylene C coating affect the corrosion rate of AZ31 helical stents in vitro.

2. Materials and Methods

2.1. Fabrication of Helical Stents

Details about stent fabrication using photo-chemical etching of biodegradable metal sheets have been published by our group [16–20,25]. The starting material was a rectangular sheet of AZ31 with dimensions of 250 mm × 250 mm and thickness of 250 μm, purchased from Goodfellow, USA (Oakdale, PA). The photo-chemical etching method transfers a selected pattern of the stent onto the metal sheet, followed by chemical etching. Figure 1 illustrates the photo-chemical etching procedure used in the fabrication of the AZ31 Mg ribbon. The described approach does not generate residual stress in the material during the manufacturing process. This patented process for stent fabrication is simple, affordable, and fast [18]. Furthermore, it is scalable and can produce hundreds of stents at once on a 4 ft × 6 ft Mg sheet. Finally, no post-manufacture treatment of the stent, such as welding, annealing, or etching is required.

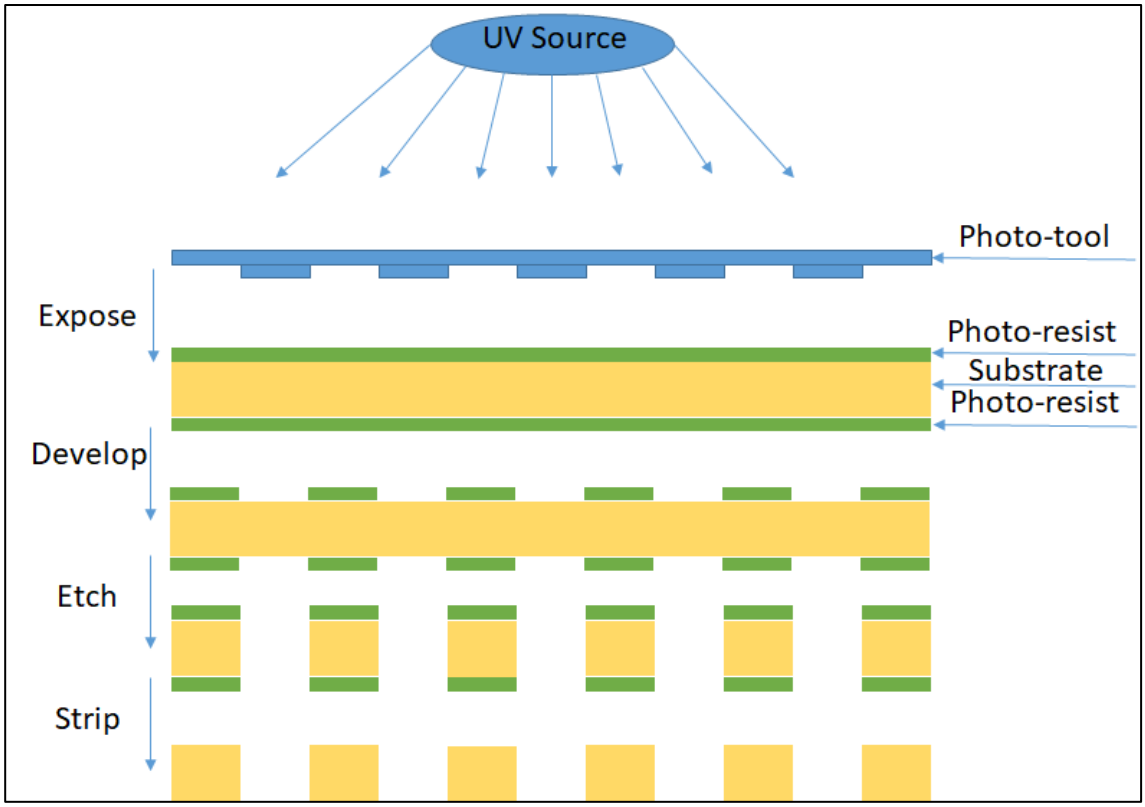

Figure1. Illustration of the photo-chemical etching method used in creating AZ31 Mg ribbons than can be made into helical stents.

A fabricated ribbon is displayed in Figure 2a. The ribbons with the desired patterns were further coiled by bending them around a metal cylinder with an appropriate diameter, to give a diameter appropriate for the stent, as displayed in Figure 2b. Helical stents with an outer diameter of 4 mm, length of 20 mm, and 21 struts were fabricated and used in this corrosion study. It expands uniformly with the help of a balloon and its appearance after expanding is shown in Figure 2c.

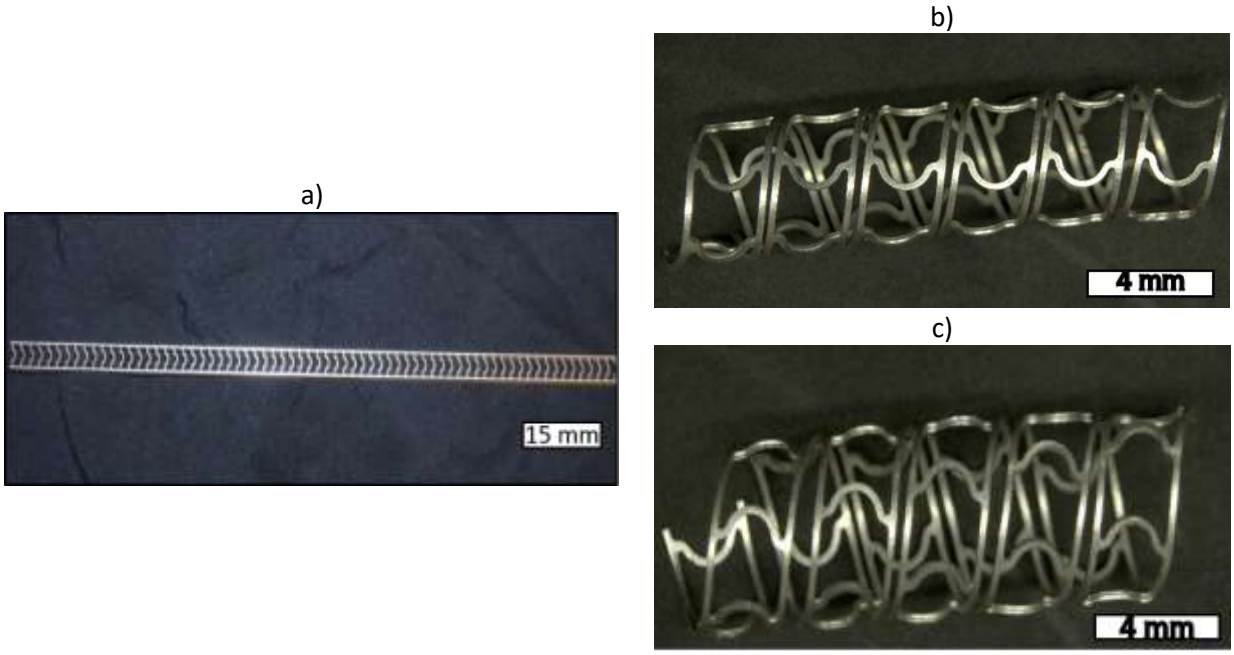

Figure 2. (a) Photo-chemically etched AZ31 Mg ribbons, as fabricated; (b) picture of unexpanded helical stent; (c) picture of balloon expanded helical stent.

2.2. Surface Modifications of AZ31 Helical Stents

2.2.1. Chemical Treatment with Inorganic Solutions

Prior to the chemical treatment, the pristine AZ31 Mg helical stents were cleaned by sonication in an ethanol bath for 2-5 minutes using an ultrasound sonicator (Fisher Scientific, Florence KY, USA). Two different inorganic solutions have been employed to conduct chemical treatment. The Inorganic solution–1 was prepared by mixing 100% nitric acid, 100% methanol, and 100% ethanol in the ratio 1:2:1, followed by stirring for 2-4 hours. The cleaned helical stents were treated in this solution for 30 seconds then blow-dried with nitrogen and rinsed in a sonicated ethanol bath for 2-5 minutes, then again blow-dried. The weight of the samples was recorded using a Sartorius microbalance after the treatment with Inorganic solution–1, which has an accuracy of 0.001 mg. Surface analysis of the treated sample was conducted by employing a Phi 5300 X-ray Photoelectron Spectrometer (XPS) with Mg K-alpha X-rays at an accelerating voltage of 15.0 kV ($h\nu = 1253.6$ eV) in a chamber maintained at 10^{-9} Torr.

The Inorganic solution–2 was prepared by mixing 85% glycerol, 65% nitric acid, and 100% acetic acid in the ratio 4:1:1, followed by stirring for 4 hours. The cleaned helical stents were treated in this solution for 1-3 minutes, then blow-dried with nitrogen and rinsed in a sonicated ethanol bath for 2-5 minutes followed by drying at 50°C in a furnace and ambient environment. The weight of the samples was recorded after performing the treatment with Inorganic solution–2.

2.2.2. Coating of Helical Stents with Parylene C

AZ31 helical stents were coated with the polymer, Parylene C, in a conformal coating

process that covered all the contours of the stent topology. It was carried out by sublimation in a Physical Vapor Deposition (PVD) chamber manufactured by Specialty Coating Systems (SCS Labcoater PDS2010, Indianapolis, IN). The sublimation process resulted in the formation of an activated polymeric Parylene C layer that uniformly coated the sample. The chemical process of sublimation, as well as the whole process of the coating formation, are described in our previous publication [17]. The preliminary step before coating the stents with Parylene C involved treatment with a silane primer solution, which served as a coupling agent. The hydroxyl groups from the silane primer solution interact with the metal surface and enhance the attachment of the Parylene C. This combination of primer and Parylene C has been reported previously to give good adhesion of the polymer coating along with mechanical and chemical robustness [26,27].

In order to evaluate the thickness of the polymer film, a flat silicon wafer partially masked with Kapton tape was placed next to the stents. After completing the Parylene C coating procedure, the Kapton tape was removed and a profilometer was used to measure the deposited film thickness. The thickness of the Parylene C can be varied by changing the initial amount of the crystalline powder dimer used, the process pressure and the evaporation temperature. The obtained conformal Parylene C coating was studied by Fourier Transform Infrared Spectroscopy (FTIR Nicolet 6700 instrument), Raman spectroscopy (Renishaw inVia instrument, with 514 nm Ar-ion laser and a laser spot of ~1 μm^2), and Scanning Electron Microscope (FEI SCIOS dual beam, 5Kv, 10KV).

2.3. In vitro study of Surface Modified Helical Stents

2.3.1. Corrosion Rate Evaluation by Weight Loss

The corrosion rate of the AZ31 stents was studied by determining the weight loss of the samples after immersion in a culture medium composed of Dulbecco's Modified Eagle's Medium (DMEM) with 10% FBS (fetal bovine serum [28]) and 1% antibiotics (10,000 units/ml penicillin and 10,000µg/ml streptomycin). This medium has electrolytic components that mimic blood and extracellular fluids. The samples included: (i) control (pristine), (ii) Inorganic solution–1 treated stents, (iii) Inorganic solution–2 treated stents, (iv) unexpanded Parylene C coated stents, and (v) balloon-expanded Parylene C coated stents (n = 3 stents per condition). The initial weight (m_i) of the test samples was recorded. For biodegradable metals the ISO standards ISO:10993-12 [29] are not easily applied, because the degradation products alter the medium. While a volume of ~5 ml would have met the ISO standard, this resulted in an undesirable change in pH, which would both modify the medium and alter corrosion. After preliminary testing, we chose a volume of 10 ml, which did not result in a pH change. Thus, the AZ31 stent samples were placed in 10 ml of the DMEM medium and left in a cell culture environment for 72 hours (37°C, 100% humidity and 5% CO_2). After immersion, the AZ31 stents were removed and dried at room temperature. For the characterization of the corrosion products after 72 hours of immersion in corrosion solution, the stents were removed from the medium and surface morphology and chemistry were analyzed using a Scanning Electron Microscope (SEM, 5Kv, 10KV) and Energy Dispersive Spectroscopy (EDS). Then, any corrosion products were removed through a chemical cleaning procedure

described in ISO:8407-2009 [29], used for corrosion of metals and alloys. Corrosion products from the surface were removed by immersing the samples in 100% chromic acid (Fisher-Scientific, USA) for 120 seconds. After blow-drying the samples, they were sonicated in 100% ethanol for 30 seconds and then blow-dried again. The final weight (m_o) of the tested stents was recorded and the weight loss for each sample *(w)* was determined using the simple equation $w = m_i - m_o$. Then, the corrosion rate C_r of the AZ31 helical stents was calculated according to the Standard Practice for Laboratory Immersion Corrosion Testing of Metals ASTM G31-72, using the equation given below [30–32], equation 1.

$$C_r = \frac{w \times K}{T \times S \times \rho} \text{---------- (1)}$$

Where C_r is the corrosion rate (mm/year), the constant *K* is $8.76e^4$, *w* is the weight loss (g), *S* is the sample area (cm^2) exposed to the DMEM medium, *T* is the time of exposure (hours) and ρ is the density of the material (g/cm^{-3}). An average and standard deviation of three measurements were determined for all five sample groups, as stated above.

2.3.2. Corrosion Rate Evaluation by Chemical Assay

Corrosion rate evaluation by weight loss was compared to evaluation by determining Mg ion release, using a chemical assay. A dye-based, spectroscopic method based on the dye called Xlydyl blue was used for evaluating free magnesium ion concentration in the cell culture medium. This dye method was selected because of the dye's high sensitivity towards Mg^{2+} and its suitability for clinical evaluation [33]. The chemical reaction involved in this chemical assay is illustrated below in equation 2.

$$Mg^{2+} + \text{Xylidyl blue} \xrightarrow{\text{pH} \sim 11.14} \text{Purple Complex ---------- (2)}$$

The Xylidyl blue working reagent was prepared by mixing a Xylidyl blue stock with ethylene glycol-bis(β-aminoethyl ether)-N, N, N′, N′-tetraacetic acid (EGTA), Tris buffer solution (pH = 11), and water to reach the final concentration of 0.1 mM Xylidyl blue. Standards (solutions of graduated concentrations of $MgCl_2$) were prepared using the DMEM medium. The Xylidyl blue working reagent was then added into both the prepared standards and samples in a proportion of 10:1 (v/v) at room temperature and left for 1 hour to react. Next, the absorbance of the samples was measured at 520 nm using a SpectraMax M2 spectrophotometer (Molecular Devices, San Jose, CA, USA). A calibration curve was generated using the standards with known Mg^{2+}concentrations. Then, the absorbance of the samples was acquired and their Mg^{2+} concentration was calculated by interpolating the absorbance on to the calibration curve using SigmaPlot software (v13, Systat Software, Inc., San Jose, CA).

2.3.3. Characterization of the Stent Surface after In Vitro Corrosion.

The surface morphology of the helical stent changed due to corrosion after immersion in the DMEM solution. These changes have

been observed by using the SEM Scanning Electron Microscope (FEI SCIOS dual beam, 5Kv, 10KV). The elemental composition of the corrosion products formed on the surface of the stents was characterized by employing Energy Dispersive Spectroscopy (EDS).

2.3.4. Statistics

Statistics were performed using Sigmaplot (v.13, SysStatSoftware, Inc., San Jose, CA). Comparisons were analyzed using a one-way ANOVA and if results showed a p-value of < 0.05, then the Holm-Sidak multiple comparisons post hoc test was employed ($p < 0.05$ considered significant). Graphs show means and standard deviations.

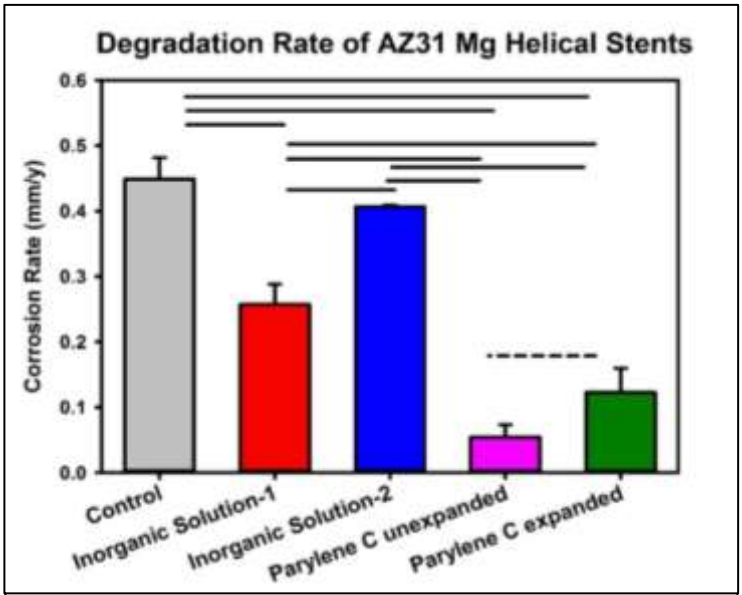

Figure 4. Corrosion rates in DMEM solution of AZ31 helical stents after surface modification by two inorganic solutions and Parylene C coating. The control in this figure represents an unexpanded and uncoated AZ31 helical stent. Bars indicate significant differences at $p < 0.05$.

3. Results

3.1. Corrosion Rate Obtained by Weight Loss

In this study, we have investigated the influence of Parylene C coating and the surface modifications using Inorganic solution–1, and Inorganic solution–2 on the corrosion rates of AZ31 Mg helical stents in DMEM solution. The results are displayed in Figure 4, where the control samples were unexpanded and uncoated AZ31 helical stents. Significant differences were detected using a one-way ANOVA, $p < 0.05$, and bars show significant differences between conditions, determined by using a Holm-Sidak post hoc test, $p < 0.05$). The unexpanded and expanded Parylene C coated stents showed a 70-85% decrease in corrosion rate when compared to the control samples. The stents treated with Inorganic solution–1 revealed a 42% decrease in

corrosion rate compared to controls. The stents treated with Inorganic solution–2 had a minor and non-significant decrease of 9% in the corrosion rate compared to controls. Comparisons revealed that the corrosion rates of the surface-modified AZ31 Mg helical stents decreased in the following order: control (0.4486 ± 0.2570 mm/year) = Inorganic solution–2 treated (0.4067 ± 0.0018 mm/year) > Inorganic solution–1 treated (0.2570 ± 0.02622 mm/year) > Parylene C coated expanded > (0.1225 ± 0.0314 mm/year) Parylene C coated unexpanded stents (0.0543 ± 0.0159 mm/year).

3.2. Corrosion Rates Obtained by Chemical Assay

The concentration of free Mg^{2+} ions in the DMEM medium, after immersing the samples in it for 72 hours at 37°C in an incubator with 5% CO_2, was measured by a Xylidyl blue dye assay and spectrophotometry. Figure 5 shows the results obtained by employing the chemical assay. Substantial differences were detected between groups using a one-way ANOVA, ($p < 0.002$) and Holm-Sidak post hoc tests. They revealed that the samples coated with Parylene C, whether expanded or not, released significantly lower Mg^{2+} ions (corroded less) compared to the control stents ($p < 0.05$). The corrosion rate for the treated devices with the inorganic solutions appeared lower, however, the differences were not significant compared to the Parylene C coated devices. This data supports the finding in Figure 4 where the Parylene C coating protected the stents the best.

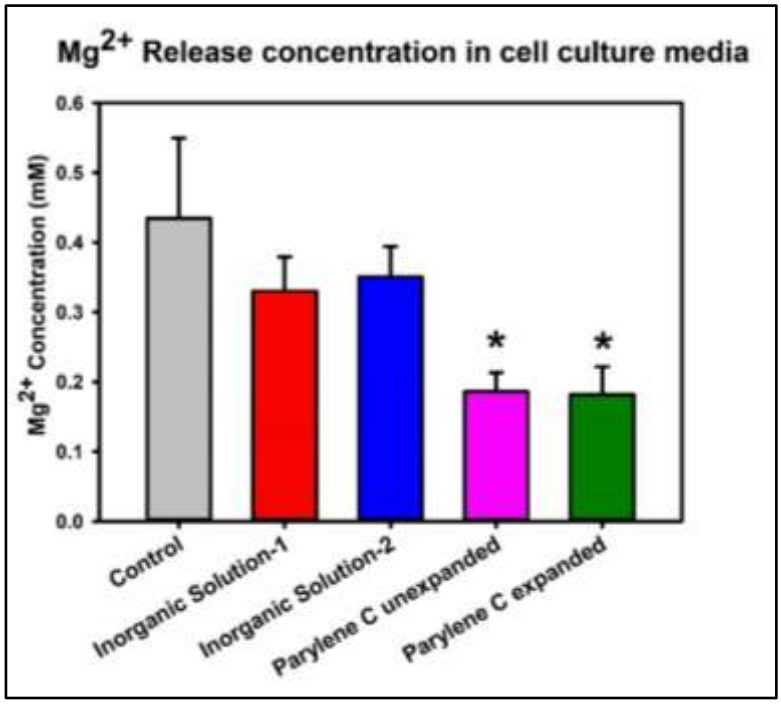

Figure 5. Comparison of Mg^{+2} ion concentrations released into the cell culture media by different surface-modified AZ31 Mg helical stents, including control (pristine AZ31), treatment in Inorganic solution–1, treatment in Inorganic solution–2, Parylene C unexpanded and expanded. (*) Significance level $p < 0.05$ compared to control.

3.3. Characterization of the Coatings on Helical Stents

3.3.1. Characterization of the Treated Stent with Inorganic Solution

Based on an XPS analysis, we found the presence of magnesium and oxygen on the surface of AZ31 helical stents after treatment with Inorganic solution-1. This suggests that magnesium oxide formation occurred during this treatment. The thickness of the magnesium oxide layer depended on the treatment time with Inorganic solution-1, as determined by XPS and illustrated in Figure 6. Besides oxygen and magnesium, the elemental analysis revealed the presence of carbon (C), which is a background element found in any of the analyzed samples. In all three samples, the concentration of magnesium increased and the concentration of the oxygen decreased with increased penetration into the sample. This is expected because the surface oxidation that took place during the treatment was a diffusion-limited process. The intersection point between the concentration profiles of magnesium and oxygen was used to determine the thickness of the formed oxide layer. From Figure 6a the thickness of the magnesium oxide on a pristine surface was found to be around 2 nm and was considered as a native oxide. For 10 second treated samples the thickness of the magnesium oxide was determined to be 15 nm, as shown in Figure 6b. By increasing the treatment time to 30 seconds the magnesium oxide layer thickness increased to 70 nm (Figure 6c). This treatment time was used to form the corrosion protection layer and study the corrosion rates displayed in Figures 4 and 5. From the results shown in Figure 6, it can be concluded that the thickness of the oxide layer can be controlled by the treatment time with Inorganic solution-1.

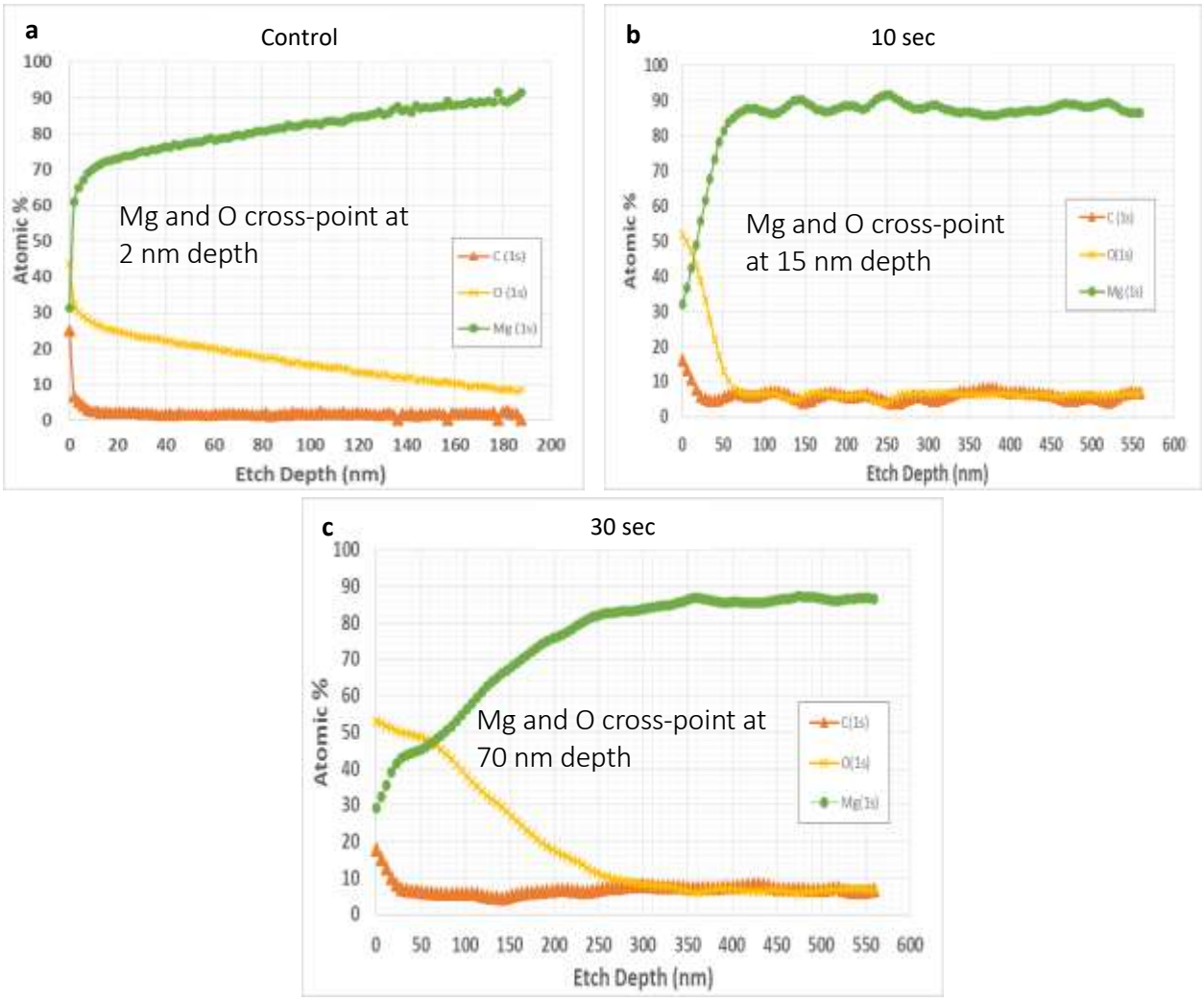

Figure 6. Depth profiles on the AZ31 surface obtained by XPS before and after treating the stent with Inorganic solution–1 for different periods of time: (a) control (pristine) stent sample; (b) sample treated for 10 seconds; (c) sample treated for 30 seconds.

3.3.2. Characterization of the Parylene C Coating

The chemical identity of the Parylene C after depositing a coating on AZ31 helical stents was characterized by Fourier Transform Infrared Spectroscopy (FTIR). This study was conducted within the wavelengths ranging from 4000 to 400 cm^{-1}. The coated ribbon was used here because of its flat surface, which allows better handling of the sample for spectra acquisition. The FTIR analysis illuminates the bonding energy of the Parylene C coating. Figure 7 compares the spectra of a Parylene C coated ribbon and pure Parylene C compound as the control. The spectra obtained at random spots 1 (Figure 7a) and 2 (Figure 7b) are identical, indicating uniform coating of the polymer. The peaks in the spectra are positioned similarly to those of the control sample (Figure 7c). Peaks at 1500–1600 cm^{-1} represent energy bands of the C=C aromatic stretching. Other peaks at 1050 cm^{-1} and 650 cm^{-1} can be assigned as the bonding energy peaks of chlorobenzene. Peaks at 1450 cm^{-1} are representative of the bonding energies of C=C and CH_2. Lastly, peaks at 2860 cm^{-1} and 2923 cm^{-1} indicate bonding energy of the

C–H bond in the methyl group and 3000 cm^{-1} designates C–H stretching [26,34–37]. This FTIR study confirmed the successful formation of a Parylene C polymeric film on the AZ31 helical stent.

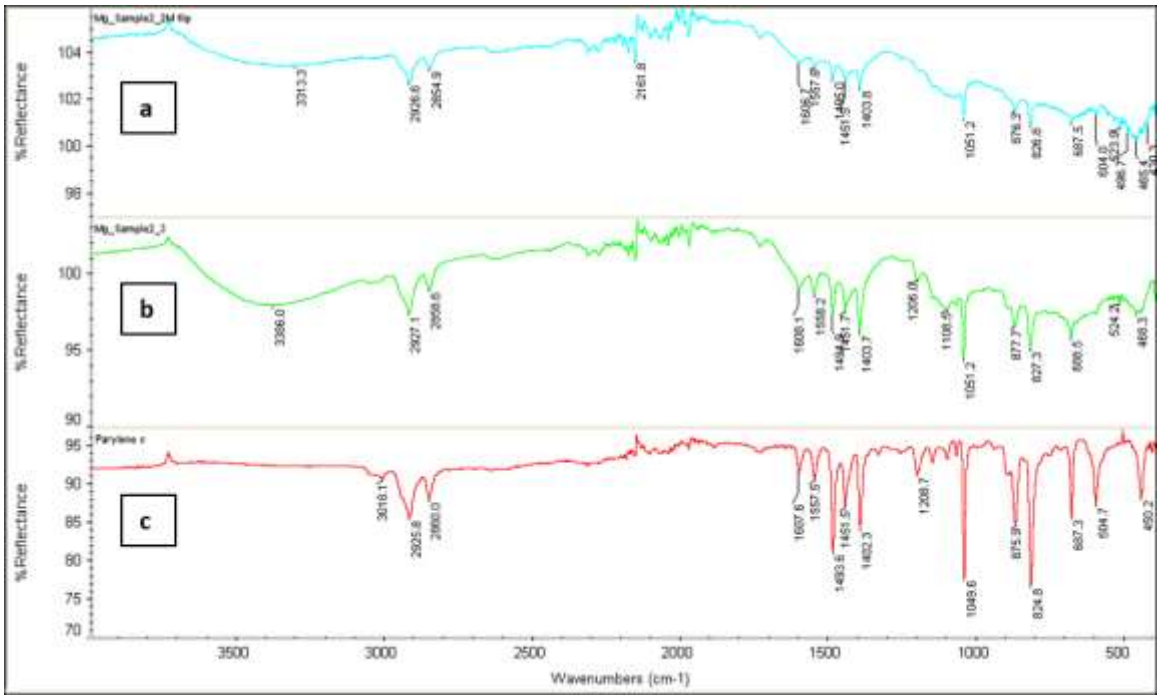

Figure 7. FTIR spectra of an AZ31 Mg ribbon coated with Parylene C and a control sample of pure Parylene Ccompound: (a) analysis conducted on a random spot 1 of the coated surface; (b) analysis conducted on a random spot 2 of the coated surface; (c) analysis conducted on a pure Parylene C sample as a control.

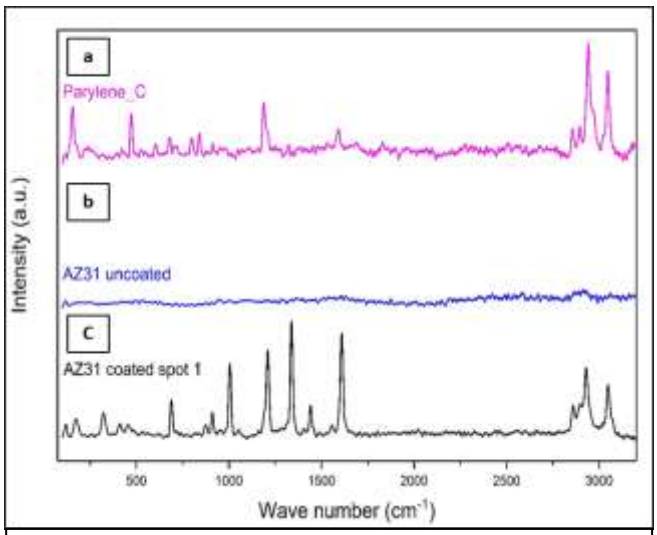

Figure 8. Raman spectroscopy of: (a) Parylene C Dimer as a control sample; (b) uncoated AZ31 Mg metal; (c) Parylene C coated stent on a random spot 1.

Raman spectroscopy with wavenumbers in the range of 3200 to 160 cm^{-1} was used to further identify the presence of Parylene C coating on the helical stent by determining the nature of the carbon bonding in the polymer groups. Here again, the tested samples were Parylene C coated AZ31 flat ribbons which allowed precise focusing of the laser on the surfaces. As illustrated in Figure 8a, characteristic peaks at 3100 cm^{-1} represent the aromatic C–H stretching, and the band between 1265–1365 cm^{-1} can be assigned to a CH in-plane deformation [38]. Figure 8b displays the spectrum of the uncoated AZ31 helical stent without any prominent peaks. Figures 8c show the spectra of Parylene C coating on AZ31 helical stents obtained by probing a random spot on the ribbon surface. The peak at 1600 cm^{-1} represents the substitution (para) of chlorine on the benzene rings, while the peaks around 1350–1500 cm^{-1} can be assigned to CH_2 twisting or C–C skeletal in-plane vibrations of the aromatic ring. The peaks within the range of 750–1000 cm^{-1} illustrate the out-of-plane deformation of CH [39]. This Raman study further proved that a Parylene C polymeric film was formed on the AZ31 helical stent.

3.4. Characterization of the Stent Surface after In Vitro Exposure

3.4.1. Morphology of the Corroded Stent Surface

The corrosion of AZ31 helical stents was assessed by observing the topography of the exposed surface after immersion in DMEM. Figure 9a displays the surface morphology obtained by SEM of the control (pristine) helical stent. Typical pitting corrosion was observed on the stent surface, which is the dominant characteristic of corroded magnesium and its alloys [6]. The Parylene C coated helical stent does not exhibit pitting corrosion on the surfaces, as shown in Figure 9b, which proves that polymer film acts as a corrosion barrier. When comparing to the controls, samples treated with Inorganic solutions 1 (Figure 9c) and 2 (Figure 9d), after immersion in DMEM, also exhibit pitting corrosion. However, the pitting was less prominent and milder compared to the control sample. This implies that the oxide layer that forms due to treatment with the inorganic solutions has reduced the impact of the corrosion.

a)

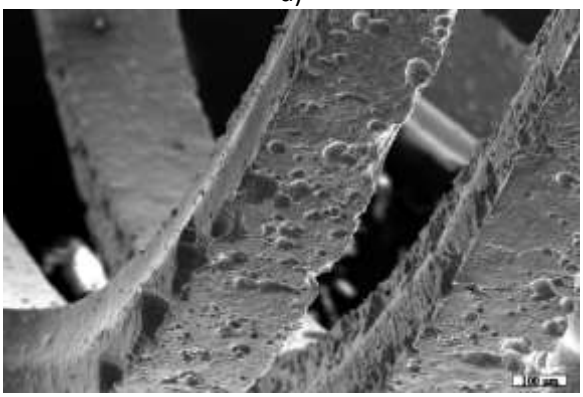

b)

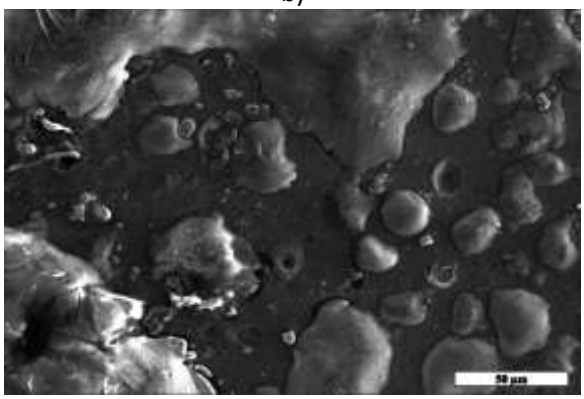

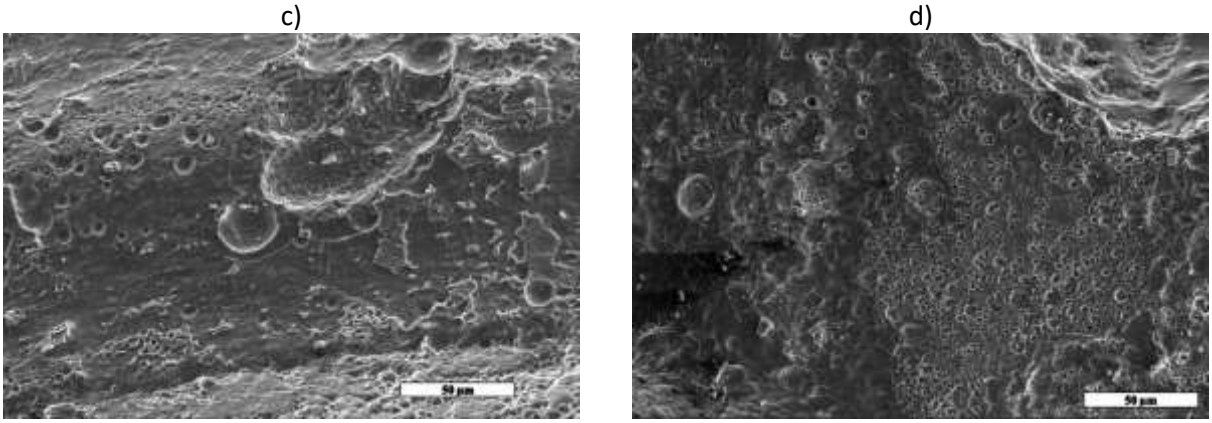

Figure 9. SEM images of AZ31 helical stents after cleaning (removing corrosion products), illustrating the formation of corrosion pits: (a) control (pristine) helical stent; (b) Parylene C coated stent; (c) stent treated with Inorganic solution–1; (d) stent treated with Inorganic solution–2. Corrosion medium is DMEM solution.

3.4.2. EDS Analysis of the Corroded Stent Surface

The exposure of the AZ31 Mg helical stent to DMEM resulted in the formation of surface corrosion products, as identified by EDS analysis. After the samples were removed from the DMEM medium, they were left to dry overnight and analyzed. The corroded surface layer consisted mainly of crystalline phosphates, carbonated and calcium-containing compounds. Figure 10a shows the SEM image of the corroded stent surface exposed to DMEM and before cleaning (removing) corrosion products. A random spot on this surface has been analyzed and the elemental analysis is displayed in Figure 10b. The elements identified within the corrosion products were O, Na, Mg, Al, Cl, P, and Ca. Magnesium and aluminum appear due to the AZ31 alloy, while the rest of the elements came from the DMEM solution. Similar observations have been reported by Xin et al. [40]. Figure 11a displays the SEM image of an uncoated AZ31 stent exposed to DMEM after cleaning the corrosion products from its surface. Typical pitting corrosion was observed. EDS analysis of a randomly selected area revealed the presence only of the elements contained in the AZ31 alloy (magnesium, aluminum, and zinc), as shown in Figure 11b.

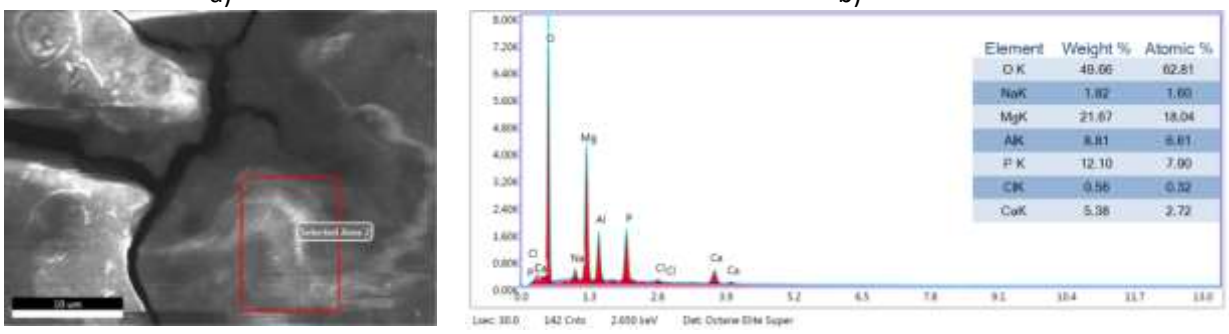

Figure 10. (a) SEM image of the uncoated AZ31 stent exposed to DMEM showing formation of corrosion products on its surface before cleaning; (b) EDS analysis of the selected area_1.

a) b)

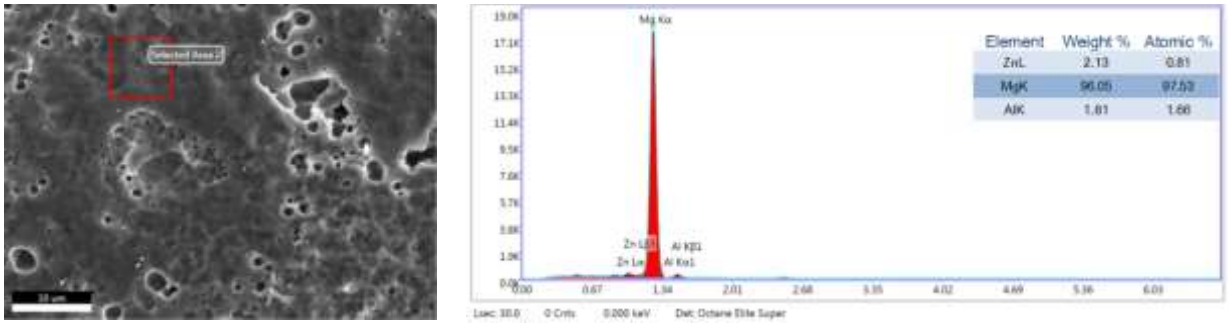

Figure 11. (a) SEM image of an AZ31, untreated stent exposed to DMEM and after cleaning off the corrosion products; (b) EDS analysis of the selected area 1.

4. Discussion

We showed here that AZ31 Mg alloy helical stents were successfully fabricated by photo-chemical etching of flat ribbons and coiling these into 3-dimensional helical devices. Surface modifications were conducted and in vitro tested to slow the corrosion rate because Mg metal would corrode rapidly when the stents are implanted and exposed to normal physiological solutions, which might compromise the device function. One method of surface modification was applying a uniform and conformal Parylene C coating, with a proven composition, which was achieved by physical vapor deposition. Other stents were treated with inorganic solutions designed to form dense and nanometer-thick magnesium oxide layers on their surfaces. After in vitro exposure of the stents for 72 hours to a cell culture medium mimicking in vivo solutions, stents coated with Parylene C showed a significant 70-85% decrease in corrosion rate when compared to control (pristine) AZ31 devices, as determined by weight loss. Using the same technique, the Inorganic solution-1 treatment resulted in a reduction in the corrosion rate of 30 - 35% compared to a control (pristine) sample, while Inorganic solution-2 treatment did not reduce corrosion rates versus the control. By employing weight loss determination of corrosion, it was possible further to find that balloon expansion of the Parylene C coated stents resulted in a higher corrosion rate compared to unexpanded coated stents. A similar effect of Parylene C and balloon expansion on corrosion rates were described in our previous publication, using Zn as a material for making biodegradable stents by photo-chemical etching [17]. As we found in [16], balloon expansion of stents may introduce defects and openings in the Parylene C coating, exposing more Mg to the solution. We also analyzed stent corrosion rates in vitro using a dye-based assay that measures the amount of free Mg ions released into the solution during corrosion. It was again demonstrated that the corrosion rates of the helical stents were significantly reduced versus control stents by applying a Parylene C coating. Using this dye-based assay, both the Parylene C coated unexpanded and expanded stents demonstrated similar corrosion rates. We believe that the balloon expansion did not introduce mechanical stress on the devices due to the unique model of expansion, which was based on uncoiling [16]. Inorganic solutions showed a modest reduction in corrosion rate compared to controls. The dye-based assay was more variable, and thereby less precise, compared

to corrosion rates determined by the weight loss measurements, presumably because solution-release of Mg ions was affected by factors such as precipitation of the Mg corrosion products out of the solution and onto the metal. These products include oxides, carbonates, and phosphates, which, upon their precipitation, will lower the concentration of Mg^{2+} in the DMEM solution. However, both methods of measurement showed that a Parylene C coating significantly reduced corrosion. Analysis of the Parylene C coating by FTIR and Raman spectroscopy confirmed the nature and the uniformity of the applied polymer. After surface treatment with Inorganic solution-1, we showed the formation of a magnesium oxide corrosion barrier with a thickness below 100 nm. Based on the treatment time we have selected the 70 nm thickness, which secured good corrosion protection without altering the mechanical properties and the dimensions of the strut. XPS analysis of the treated stents with Inorganic solution-2 was not conducted because this treatment did not provide significant corrosion protection. We believe that the oxidation power of the Inorganic solution-2 was not strong enough, due to the presence of the viscous glycerol, to produce a dense magnesium oxide that could protect the stent. Further analysis by SEM and EDS of the corroded surfaces of the stents brought us to the conclusion that the corrosion propagated in the metal occurred through pitting for the controls and stents treated with Inorganic solution-2. However, the morphology of the corroded surface coated with Parylene C did not reveal any corrosion pits, which therefore explains why this coating provides greater corrosion resistance.

5. Conclusions

The results obtained in this study are encouraging for further in vivo testing of AZ31 Mg helical stents with Parylene C coatings, particularly for tissue engineering. It was found that the coating slowed corrosion, thus retaining the physical strength of the implant for longer time periods, which is important for successful healing.

Acknowledgments

The authors would like to acknowledge the financial support provided by the NSF ERC for Revolutionizing Biomaterials through grant EEC-EEC-0812348. FTIR spectra were obtained with the assistance of Mr. Necati Kaval from the Department of Chemistry at the University of Cincinnati and his help is appreciated.

References

1. AL-Mangour B, Mongrain R, Yue S. Coronary Stents Fracture: An Engineering Approach (Review). *Mater Sci Appl*. 2013;04(10):606-621. doi:10.4236/msa.2013.410075
2. Bedoya J, Meyer CA, Timmins LH, Moreno MR, Moore JE. Effects of Stent Design Parameters on Normal Artery Wall Mechanics. *J Biomech Eng*. 2006;128(5):757. doi:10.1115/1.2246236
3. Kastrati A, Mehilli J, Dirschinger J, et al. Restenosis after coronary placement of various stent types. *Am J Cardiol*. 2001;87(1):34-39. doi:10.1016/S0002-9149(00)01268-6
4. Walker J, Shadanbaz S, Kirkland NT, et al. Magnesium alloys: Predicting in vivo corrosion with in vitro immersion testing. *J Biomed Mater Res - Part B Appl Biomater*. 2012;100 B(4):1134-1141. doi:10.1002/jbm.b.32680
5. Witte F, Hort N, Feyerabend F, Vogt C. Corrosion of Magnesium Alloys. In: *Corrosion of Magnesium Alloys , (Ed: G. Song), Woodhead , Philadelphia, PA, USA 2011*. ; 2008:403.
6. Xin Y, Hu T, Chu PK. In vitro studies of biomedical magnesium alloys in a simulated physiological environment: A review. *Acta Biomater*. 2011;7(4):1452-1459. doi:10.1016/j.actbio.2010.12.004
7. Vormann J. Magnesium: Nutrition and metabolism. *Mol Aspects Med*. 2003;24(1-3):27-37. doi:10.1016/S0098-2997(02)00089-4
8. Zeng R, Dietzel W, Witte F, Hort N, Blawert C. Progress and challenge for magnesium alloys as biomaterials. *Adv Eng Mater*. 2008;10(8):3-14. doi:10.1002/adem.200800035
9. Frazin LJ, Lanza G, Vonesh M, et al. Functional chiral asymmetry in descending thoracic aorta. *Circulation*. 1990;82(6):1985-1994. doi:10.1161/01.CIR.82.6.1985
10. Stonebridge PA, Brophy CM. Spiral laminar flow in arteries ? Erythropoietin and spontaneous platelet aggregation in haemodialysis patients. *Lancet*. 1991;338:1360-1361.
11. SEGADAL L, MATRE K. Blood velocity distribution in the human ascending aorta. 2000:2000.
12. T K, HL G, M M, S M, Y S. Flow patterns in vessels of simple and complex geometries. In: Leonard EF, Turitto VT, Vroman L, eds. Blood in contact with natural and artificial surfaces. In: *New York: Academy Press,*. ; 1987:422-441.
13. Caro CG, Seneviratne A, Heraty KB, et al. Intimal hyperplasia following implantation of helical-centreline and straight-centreline stents in common carotid arteries in healthy pigs: Influence of intraluminal flow. *J R Soc Interface*. 2013;10(89):1-8. doi:10.1098/rsif.2013.0578
14. Zeller T, Gaines PA, Ansel GM, Caro CG. Helical centerline stent improves patency: Two-year results from the randomized mimics trial. *Circ Cardiovasc Interv*. 2016;9(6):1-8. doi:10.1161/CIRCINTERVENTIONS.115.002930
15. Wholey MH, Finol EA. Designing the ideal stent. In: *Endovascular Today*. ; 2007:25–34.
16. Koo Y, Tiasha T, Shanov VN, Yun Y. Expandable Mg-based Helical Stent Assessment using Static, Dynamic, and Porcine Ex Vivo Models. *Sci Rep*. 2017;7(1):1-10. doi:10.1038/s41598-017-01214-4

17. Kandala BSPK, Zhang G, Hopkins TM, An X, Pixley SK, Shanov V. In vitro and in vivo testing of zinc as a biodegradable material for stents fabricated by photo-chemical etching. *Appl Sci*. 2019;9(21). doi:10.3390/app9214503
18. Shanov VN, Roy-Chaudhury P, Schulz M, Yin Z, Campos-Naciff B, Wang Y. Making Magnesium Biodegradable Stent for Medical Implant Applications, US Patent 9,655,752, May 23, 2017. 2013;(12).
19. Ye SH, Chen Y, Mao Z, et al. Biodegradable Zwitterionic Polymer Coatings for Magnesium Alloy Stents. *Langmuir*. 2019;35(5):1421-1429. doi:10.1021/acs.langmuir.8b01623
20. Coyan GN, D'Amore A, Matsumura Y, et al. In vivo functional assessment of a novel degradable metal and elastomeric scaffold-based tissue engineered heart valve. *J Thorac Cardiovasc Surg*. 2019;157(5):1809-1816. doi:10.1016/j.jtcvs.2018.09.128
21. Gu X, Mao Z, Ye S-H, et al. Biodegradable, elastomeric coatings with controlled anti-proliferative agent release for magnesium-based cardiovascular stents. *Colloids Surf B Biointerfaces*. 2016;144:170-179. doi:10.1016/j.colsurfb.2016.03.086
22. D E, McBRIDE MD. ABSORBABLE METAL IN BONE SURGERY. *J Am Med Assoc*. 1938;278(Dec 31).
23. VV T, DN T. The resorbing metallic alloy 'Osteosinthezit' as material for fastening broken bone. *Khirurgiia 1944*. 8:41–4.
24. Witte F, Kaese V, Haferkamp H, et al. In vivo corrosion of four magnesium alloys and the associated bone response. *Biomaterials*. 2005;26(17):3557-3563. doi:10.1016/j.biomaterials.2004.09.049
25. Wang J, Giridharan V, Shanov V, et al. Flow-induced corrosion behavior of absorbable magnesium-based stents. *Acta Biomater*. 2014;10(12):5213-5223. doi:10.1016/j.actbio.2014.08.034
26. Kahouli A, Sylvestre A, Ortega L, et al. Structural and dielectric study of parylene C thin films. *Appl Phys Lett*. 2009;94(15). doi:10.1063/1.3114404
27. Cieślik M, Engvall K, Pan J, Kotarba A. Silane-parylene coating for improving corrosion resistance of stainless steel 316L implant material. *Corros Sci*. 2011;53(1):296-301. doi:10.1016/j.corsci.2010.09.034
28. Spiro RG. Studies on Fetuin, a Glycoprotein of Fetal Serum. *J Biol Chem*. 1960;235(10):2860-2869.
29. International standard ISO 8407. *ISO 10993-12*.; 2009.
30. Liu L, Meng Y, Dong C, Yan Y, Volinsky AA, Wang LN. Initial formation of corrosion products on pure zinc in simulated body fluid. *J Mater Sci Technol*. 2018;34(12):2271-2282. doi:10.1016/j.jmst.2018.05.005
31. ASTM. Standard Practice for Laboratory Immersion Corrosion Testing of Metals. In: *Annual Book of ASTM Standards, Philadelphia, PA, 2011*. ASTM International; 2011:2011.
32. Ibrahim H, Klarner AD, Poorganji B, Dean D, Luo AA, Elahinia M. Microstructural, mechanical and corrosion characteristics of heat-treated Mg-1.2Zn-0.5Ca (wt%) alloy for use as resorbable bone fixation material. *J Mech Behav Biomed Mater*. 2017;69(January):203-212. doi:10.1016/j.jmbbm.2017.01.005
33. Chromy V, Svoboda V, Stepanova I. Spectrophotometric in Biological Determination Fluids with Xylidyl of Magnesium. *Biochem Med*.

1973;217:208-217.
34. Surmeneva MA, Vladescu A, Cotrut CM, et al. Effect of parylene C coating on the antibiocorrosive and mechanical properties of different magnesium alloys. *Appl Surf Sci*. 2018;427:617-627. doi:10.1016/j.apsusc.2017.08.066
35. Lee T, Lee J, Park C. Characterization of parylene deposition process for the passivation of organic light emitting diodes. *Korean J Chem Eng*. 2002;19(4):722-727. doi:10.1007/BF02699324
36. Bera M, Rivaton A, Gandon C, Gardette JL. Comparison of the photodegradation of parylene C and parylene N. *Eur Polym J*. 2000;36(9):1765-1777. doi:10.1016/S0014-3057(99)00259-1
37. Song JS, Lee S, Jung SH, Cha GC, Mun MS. Improved Biocompatibility of Parylene-C Films Prepared by Chemical Vapor Deposition and the Subsequent Plasma Treatment. *J Appl Polym Sci*. 2010;116(5):2658-2667. doi:10.1002/app
38. Balss KM, Llanos G, Papandreou G, Maryanoff CA. Quantitative spatial distribution of sirolimus and polymers in drug-eluting stents using confocal Raman microscopy. *J Biomed Mater Res - Part A*. 2008;85(1):258-270. doi:10.1002/jbm.a.31535
39. Mathur MS, Weir A. Laser Raman and Infrared Spectrum of Poly-p-Xylylene. *J Mol Struct*. 1973;15:459-463.
40. Xin Y, Huo K, Hu T, Tang G, Chu PK. Corrosion products on biomedical magnesium alloy soaked in simulated body fluids. *J Mater Res*. 2009;24(8):2711-2719. doi:10.1557/jmr.2009.0323

